WEDNESDAY SLIDE CONFERENCE 2012-2013

Conference 16

27 February 2013

**CASE I:** PA5003 (JPC 4017810).

Signalment: Adult (age unspecified), male, rhesus monkey *(Macaca mulatta)*.

History: This adult male rhesus macaque had been infected 7 months previously with SIV and had a marked decrease in its CD4 cell counts. Prior baseline (pre-SIV infection) CT imaging had revealed a small, circumscribed, spherical, thick-walled air-filled cavitary lesion in the left lower lung lobe which had recently markedly expanded in size and was now associated with some adjacent parenchymal consolidation. An acid-fast organism was recovered from a recent gastric aspirate, although further identification/speciation was not performed. The animal was humanely sacrificed
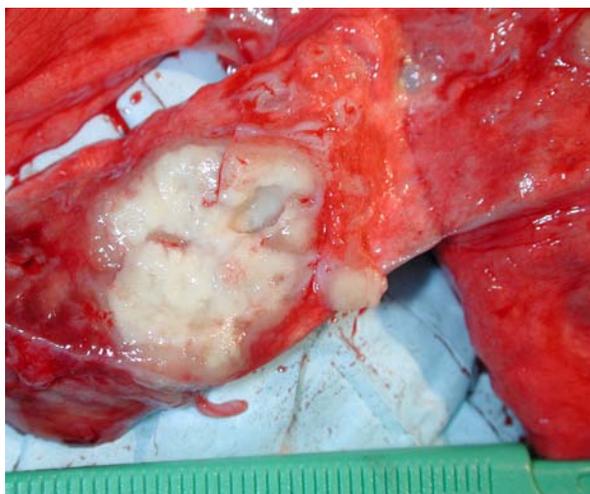

1-1. At autopsy, there were marked fibrous adhesions between the left lower lobe and the diaphragmatic and lateral thoracic wall. Dissection revealed a well-demarcated are of necrosis and cavitation as seen here. (Photo courtesy of: The Division of Laboratory Animal Resources, S 1040 Biomedical Science Tower, University of Pittsburgh, Pittsburgh, PA 15668; http://www.dlar.pitt.edu/)
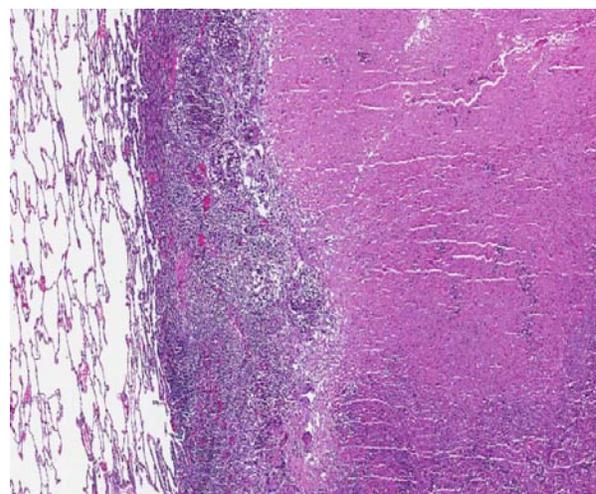
1-2. Lung, rhesus monkey: A large peribronchiolar pyogranuloma replaces up to 50% in some sections. (HE 40X)

1
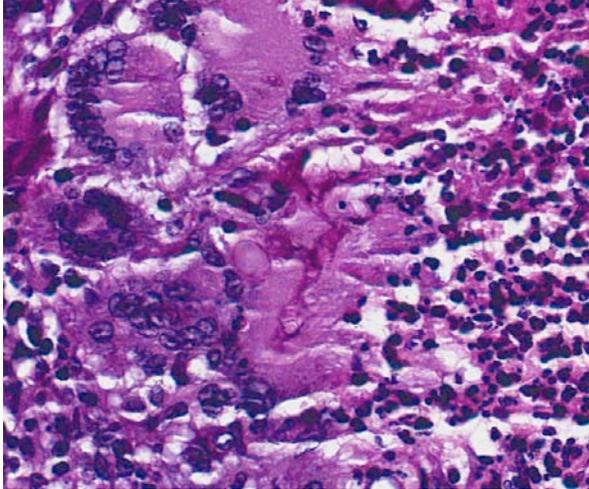
1-3. Lung, rhesus monkey: At the periphery of the pyogranuloma, fungal hyphae with non-parallel walls measuring up to 12 μm in diameter are present within multinucleated macrophages of both the foreign body and Langhans' types. As is occasionally the case with zygomycete fungi, the hyphae in this case stain more prominently with hematoxylin and eosin than with silver stains. (HE 400X)
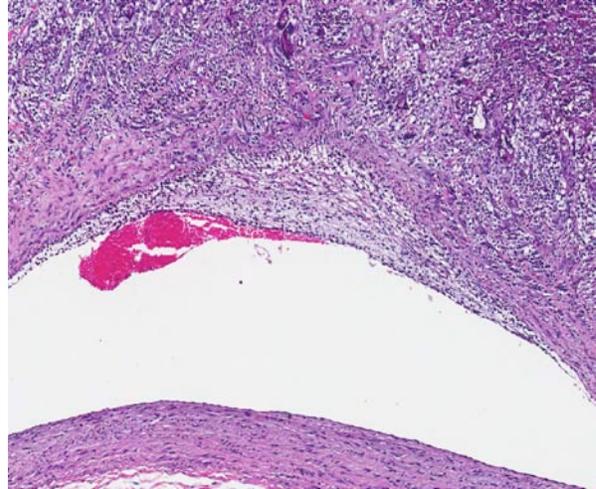
1-4. Lung, rhesus monkey: There is a focally extensive granulomatous arteriolitis resulting from local extension of the pyogranuloma into an adjacent arteriole. (HE 400X)

and presented immediately for post-mortem examination.

Gross Pathology: In the superior portion of the left lower lobe at the reflection of the anterior and posterior surfaces, there was a 3.5-4 cm area of firmness with associated marked fibrous adhesions to adjacent diaphragmatic and lateral thoracic wall surfaces. Some plum discoloration was noted in lung parenchyma superior to the lesion. On palpation the structure was somewhat softer centrally. On mid-central transection along the long axis there were small irregular areas of central cavitation within a large cream-colored necrotic core with a caseous texture. Peripherally, there was margination by an irregular, variable thickness rim of grey connective tissue. When excised in a para-sagittal plane there were multiple & coalescing small satellite nodules visible, generally with a similar appearance, although with less overt central necrosis. In the proximal portion of the right upper lobe, just distal to the hilum, there was a large (approximately 1.5 cm) nodular area of parenchymal firmness that was similar in transected appearance to the LLL lesion. No other areas of nodularity or consolidation were observed or palpated in other lung regions.

Clusters of enlarged, plump-appearing thoracic lymph nodes were present, especially in the left and right subclavicular and superior paratracheal regions. On transection, these showed partial effacement of normal cortical-medullary nodal architecture with cream-colored homogeneous tissue. However, no definitively recognizable granuloma structures were observable within them. Approximately 75% of the liver effaced by multifocal and coalescing expansile cream-colored solid but soft nodules. These ranged in size from several millimeters to several centimeters (coalescences). The spleen was enlarged to approximately 4 to 5 times its normal size. Visible centrally within the body was a 3 to 4 cm cream-colored soft mass. This lesion was mottled and soft centrally, suggesting early avascular necrosis. Other smaller solid cream colored masses were present within the splenic parenchyma. The right adrenal gland was massively enlarged (3 to 4 cm) and totally effaced by a similar appearing homogeneous cream colored mass and a 2 cm mass was present in the caudal pole of the right kidney. A large portion of one of the poles of the left adrenal gland was also replaced by a solid, grey-colored mass. Mesenteric lymph nodes were markedly enlarged, homogeneous and without normal-appearing central architecture. The GI tract was considered unremarkable grossly. No lesions were noted in the remainder of the abdominal viscera. Inguinal and axillary lymph nodes were enlarged 2-3 times normal size and had an appearance on cut surface similar to that described for the thoracic lymph nodes examined.

Laboratory Results: An acid-fast organism had been recently isolated from a gastric aspirate sample although it was not further speciated.

Histopathologic Description: The cavitary lung lesion consists of a massively ectatic and largely destroyed bronchus, as evidenced by the residual fragmented foci of bronchial wall (not visible in all slides). Filling this structure are massive amounts of amorphous, eosinophilic necrotic debris with evidence of early collagen fibril formation within. Easily visible in many areas are large numbers of fungal organisms. These structures are very pleomorphic, with broad, hyaline, ribbon-like, wide-angled branching, pauciseptate irregular hyphae. They often appear as large dilated structures, sometimes with central granular or vacuolated spherical content. Inflammation is abundant, especially along the margins of the cavity and is granulomatous or pyogranulomatous in nature, consisting of large multinucleated giant cells, macrophages, degenerative neutrophils, eosinophils and a prominent but irregular margin of lymphoplasmacytic cells.

Contributor's Morphologic Diagnosis: Necrotizing granuloma(s), focally extensive or multifocal (depending on slide), with numerous visible hyphae, present within an extensively effaced and dilated bronchus (visible in some sections).

Contributor's Comment: A primary differential in this case of an SIV immunosuppressed animal with a cavitary lung lesion and isolation of an acid-fast organism on gastric aspiration (GA) was tuberculosis. Cultures of the lung lesions were negative for all *Mycobacterium* species including *M. tuberculosis,* although the monkey was positive for *M. avium* on Prmagam assay and the acid fast organism identified via GA likely originated from the gut. Concurrent disseminated lymphoma accounted for the enlargement and effacement of thoracic and peripheral lymph nodes as well as liver, spleen, kidney and adrenal lesions. Although frank, solid regions of lymphoma were not noted within lung, some of the lymphoid infiltrates surrounding the necrotizing granuloma(s) and in bronchial & vascular associated lymphoid tissue had a prominent component of more blastic appearing cells.

Pulmonary cavities are frequent manifestations of a wide variety of inflammatory processes involving the lung and considerable variation exists in the pathophysiology of their development. The term itself (cavity) has somewhat different pathological and radiological definitions, generally connoting air/gas filled spaces with definable walls of various thicknesses.[9] Other related and overlapping terms include lung abscess (a necrotizing lung infection characterized by pus or other inflammatory material filled cavity) and pulmonary mycetoma. The latter somewhat dated term is occasionally used to reference a fungal ball within a pre-existing lung cavity, although the designation mycetoma more properly refers to a chronic subcutaneous infection caused by actinomyces or fungus. In humans the list of conditions leading to cavitation is extensive.[3] Non-infectious entities potentially resulting in lung cavities include malignancies, rheumatologic diseases (especially Wegener's granulomatosis) and pulmonary infarction and necrosis. A variety of common bacterial infections (*S. pneumonia, H. influenza, Klebsiella pneumoniae*, etc) can cause cavitary pneumonias as well as less common agents such as *Nocardia, Actinomycosis, Burkholderia* (Melioidosis) and *Rhodococcus*. Mycobacterium, both tuberculous and non-tuberculous, are widely known to lead to cavitary change; in fact, *Mycobacterium tuberculosis* generally has the highest prevalence of cavities among persons with pulmonary disease of any infection.[3] Of parasitic causes of lung cavitation, *Echinococcus* and *Paragonimus* are the most commonly mentioned. Fungal etiologies also abound and include *Aspergillus* (often arising as fungal balls within a pre-existing cavity), *Histoplasma*, *Blastomyces*, *Coccidioides*, and *Pneumocystis*.

The fungus causing infection in this animal was identified by culture as *Cunninghamella bertholletiae*. This saprophytic, filamentous species is found primarily in soil and is one member of the *Zygomycetes* class of fungi, diseases from which are broadly referred to as zygomycosis.[2] Molds in this class are comprised of two fungal groups of primary medical importance – the orders *Mucorales* and *Entomophthorales*. Infections caused by *Mucorales* were formerly termed phycomycosis, a term no longer used.[7] *C. bertholletiae* is classified under this order and is the only member of its genus proven to be pathogenic. It has been increasingly reported as an emerging pathogen[4] causing disease in a wide range of immunosuppressed human patients with debilitating factors usually related to diabetes mellitus, corticosteroid treatment or granulocytopenia. Interestingly, T-cell dependent immunity does not play an essential role in the defense of this infection and AIDS patients are not particularly susceptible to these organisms.[5] Infection with *Cunninghamella* has rarely been reported in immunocompetent hosts.[10]

Although spontaneous zygomycosis is recognized not uncommonly in a variety of species,[8] naturally occurring *Cunninghamella* infections are not as widely reported in animals. However, murine models of the disease have been developed.

Whether the monkey in this case had a pre-existing primary cavitary lung lesion of some other pathogenesis (e.g. Trematode parasite, acariasis, etc) which subsequently became colonized after immunosuppression with this zygomycosis or the *Cunninghamella* arrived in conjunction with a primary cavity forming insult and remained contained until SIV infection is not clear – nor will the exact series of events ever be ascertainable. There was no morphological or culture evidence of concurrent infectious or parasitic agents.

JPC Diagnosis: Lung: Pyogranuloma, focally extensive, with fungal hyphae, rhesus monkey (*Macaca mulatta*), primate.

Conference Comment: As the contributor states in their excellent summary of *Cunninghamella bertholletiae*, naturally occurring infections with this zygomycete fungus are uncommon in animals, despite the ubiquitous nature of these fungi. In a recent report, the first case of *C. bertholletiae* in a marine mammal occurred in a 28-year-old female captive killer whale that died after a three-month history of gastrointestinal disease. Necropsy findings included numerous variably-sized rocks in the gastric compartments associated with ulceration, tubercule-like lesions in the lungs and multiple abscesses in the pulmonary cavities. Microscopic examination revealed suppurative pneumonia associated with fungal hyphae and numerous bacterial colonies. *Cunninghamella bertholletiae*, as well as *Proteus mirabilis, Pseudomonas aeruginosa and Pseudomonas oryzihabitans* was cultured from the lesions. It is presumed this whale's infection with these opportunistic pathogens was secondary to immunosuppression, and it is hypothesized that the gastric lesions may have played a role in facilitating mycotic proliferation.[1]

In humans, *C. bertholletiae* has been shown to exhibit a higher pathogenicity and a poorer prognosis than infections with other members of the order *Mucorales*, specifically *Rhizopus* and *Mucor* species.[6] Neutrophils play an important role in the clearing of *C. bertholletiae* infection; thus its resistance to neutrophil-induced damage via IL-8 suppression accounts in part for its increased virulence. IL-8 is a potent chemotactic factor and thus its suppression results in a decrease in the number of neutrophils recruited. Other mechanisms of neutrophil suppression, including resistance to iron chelation, fungal mass, and modulation of TNF-alpha related responses, appear to enhance the virulence of this interesting zygomycete.[6]

Contributing Institution: Division of Laboratory Animal Resources
S 1040 Biomedical Science Tower
University of Pittsburgh
Pittsburgh, PA 15668
http://www.dlar.pitt.edu/

References:
1. Abdo W, Kakizoe Y, Ryono M, Dover SR, Fukushi H, Okuda H, et al. Pulmonary zygomycosis with *Cunninghamella* bertolletiae in a killer whale *(Orcinus orca). J. Comp Pathol.* 2012;147(1):94-99.
2. Chayakulkeeree M, Ghannoum MA, Perfect JR. Zygomycosis: the re-emerging fungal infection. *Eur J Clin Microbiolo Infect Dis*. 2006;25:215-229.
3. Gadkowski LB, Stout JE. Cavitary pulmonary disease. *Clinical Microbiol Rev*. 2008;21(2): 305-333.
4. Honda A, Kamei K, Unno H, Hiroshima K, Kuriyama TA. Murine model of zygomycosis by *Cunninhamella* bertholletiae. *Mycopathologia*. 1999;144:141-146.
5. Kamei K. Animal models of zygomycosis – *Agsidia, Rhizopus, Rhizomucor* and *Cunninhamella*. *Mycopathologia*. 2000;152:5-13.
6. Gomes MZR, Lewis RE, Kontoyiannis DP. Mucormycosis caused by unusual mucormycetes, non-*Rhizopus*, -*Mucor*, and -*Lichtheimia* species. *Clin Microbiol Rev*. 2011;24(2):411–445.
7. Migaki G, Schmidt RE, Toft JF, Kaufmann AF. Mycotic infections of the alimentary tract of nonhuman primates: a review. *Vet Pathol*. 1982;19:93-103.
8. Sondhi J, Gupta P, Sood N. Experimental zygomycosis in rabbits: clinicopathological studies. *Mycopathologia*. 1999;144:29-37.
9. Tuddenham WJ. Glossary of terms for thoracic radiology: recommendations of the nomenclature committee of the Fleischner society. *Am J Roentgenol*. 1984;143:509-517.
10. Zeilender S, Drenning D, Glauser FL, Bechard D. Fatal Cunninghamella bertholletia in an immunocompetent patient. *Chest 97*. 1990;1482-1483.

CASE II: 64354 (JPC 4019873).

Signalment: Two dams (seven- and four- month-olds) and three pups (one- month -olds), all females, NOD SCID Gamma (NOD.Cg-*Prkdc^{scid} Il2rg^{tm1Wjl}*/SzJ; NSG), mice (*Mus musculus*).

History: Two-month history of high pup mortality and alopecia in NOD.Cg-*Prkdc^{scid} Il2rg^{tm1Wjl}*/SzJ (NSG) mice. Original NSG mice purchased from Jackson Laboratory about one year previously had produced litters. Their offspring (F1 generation) also bred successfully; however, their pups (F2) developed alopecia at two weeks old, and had significant preweaning mortality. The few surviving pups eventually regrew hair at five to six weeks old and were used for breeding. Two breeding females from this second generation (F2), ages four and seven months, and three pups, all one month old, were submitted to Johns Hopkins Diagnostic Veterinary Pathology Service to evaluate the pup morbidity and mortality.

Gross Pathology: Gross examination of the pups and dams revealed variable, multifocal to coalescing, mild to marked alopecia over the dorsum, ventrum and face. The underlying skin was grossly normal, without obvious hyperkeratosis (flaking or scaly skin), erythema, or ulceration. No other gross abnormalities were identified in the pups.

2-1. Haired skin, NSG mouse: Affected mice exhibit variable alopecia over the dorsum, ventrum and face. The underlying skin was grossly normal, without obvious hyperkeratosis, erythema, or ulceration. (Photo courtesy of: The Department of Molecular and Comparative Pathobiology, Johns Hopkins University, School of Medicine, 733 N. Broadway St., Suite 811, Baltimore, MD 21205; http://www.hopkinsmedicine.org/mcp/index.html)

Dam A (4 months old, 25.2 g) and Dam B (7 months old, 20.73 g), were in thin body condition, and had splenomegaly (0.13 and 0.18 g respectively). Dam B also had a grossly visible anterior mediastinal mass, approximately 1cm diameter, in the region of the thymus, with deep invasion into mediastinum and along parietal pleura.

Laboratory Results: A PCR Rodent Infectious Agents (PRIA) panel was performed on pooled feces, skin and oropharyngeal swabs from the dams and three pups, and was positive for *Corynebacterium bovis* and *Staphylococcus xylosus*. This panel tests for over 35 common mouse microbial agents, including viruses, parasites, bacteria, and fungi.

Automated complete blood counts (CBC) were performed on Dams A and B and are displayed in the included chart.

	Dam A	Dam B
WBC (K/µl)	4.44	22.8
NE (K/µl)	2.64	12.8
Ly (K/µl)	0.99	4.11
Eo (K/µl)	0.25	1.79
Ba (K/µl)	0.02	0.17
Mo (K/µl)	0.54	3.92
RBC (M/µl)	7.91	10.44
PLT (K/µl)	800	440

Histopathologic Description: Skin (from Dam B): Sparsely haired, non-pigmented skin. Diffusely, there is marked orthokeratotic hyperkeratosis, and multifocal small, ~10 µm, 'dusty' intracorneal bacterial colonies within follicles and in superficial keratin. The bacteria are very small basophilic coccobacilli. Multifocally, there is mild but conspicuous thickening of the stratum spinosum up to 5 cell layers (acanthosis), and the superficial dermis contains low numbers of lymphocytoid mononuclear cells.

Transverse section of head, decalcified (from Dam A): Expanding the bone marrow and spilling out into the adjacent subdural space and meninges, and ventrally surrounding the pituitary and cranial nerves, is an unencapsulated, poorly delineated, neoplastic cellular infiltrate consisting of a monomorphic population of round cells (lymphocytes) multifocally coalescing into densely cellular sheets. Cytomorphology is somewhat compromised by demineralization of the head
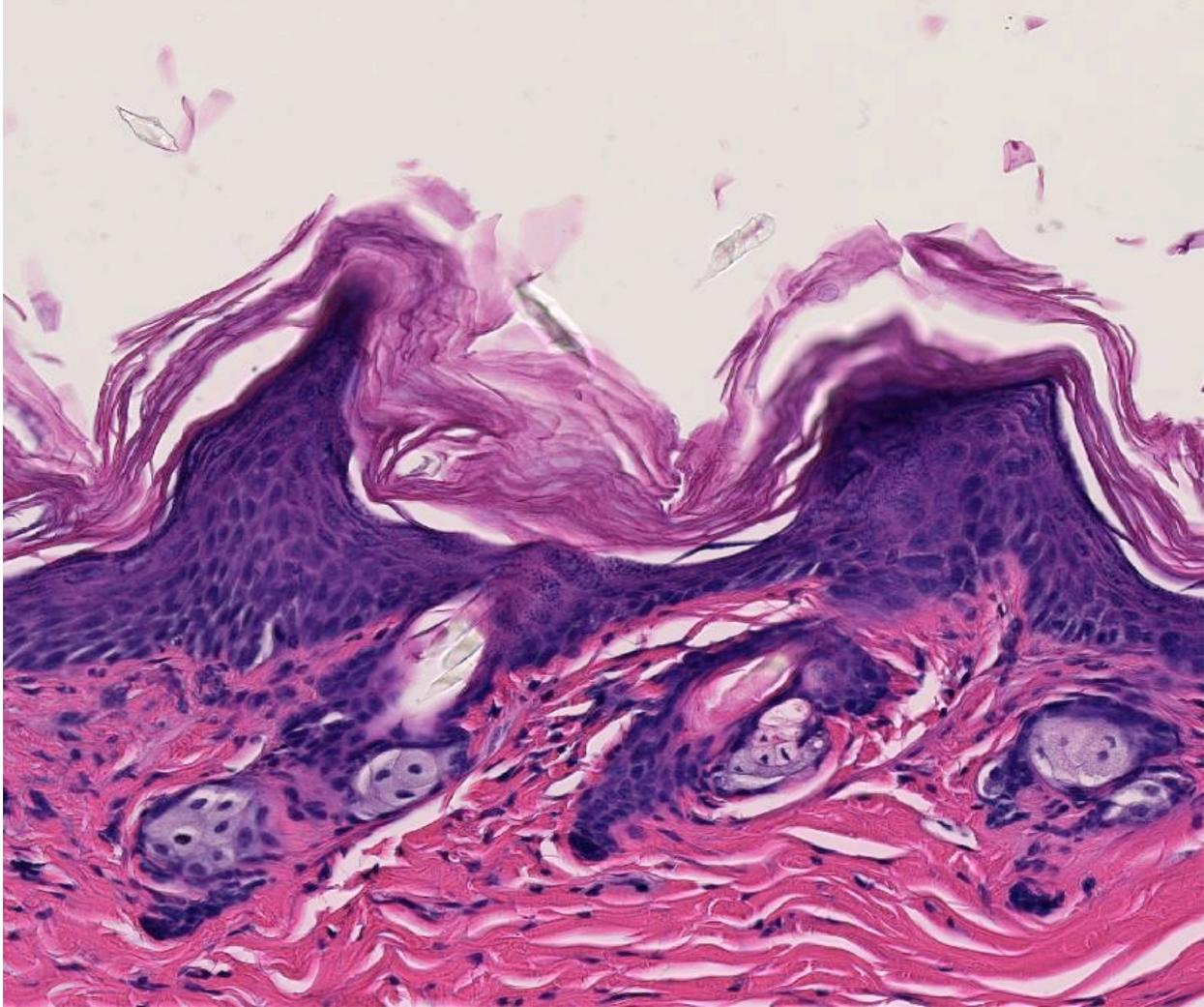
2-2. Haired skin, NSG mouse: There is diffuse epidermal hyperplasia with marked orthokeratotic hyperkeratosis. (HE 320X)

specimen; however, neoplastic lymphocytes are characterized by distinct cell borders, a moderate amount of eosinophilic granular cytoplasm, a round to oval centrally located nucleus, stippled chromatin, and occasionally 1-2 indistinct nucleoli. Mitoses are 0-1/HPF, and anisocytosis and anisokaryosis are minimal. There is multifocal minimal hemorrhage, and mild individual cell necrosis (pyknotic nuclei, and karyorrhectic debris).

Contributor's Morphologic Diagnosis: 1. Skin, dam: Hyperkeratosis, orthokeratotic, diffuse, marked with mild acanthosis, minimal non-suppurative dermatitis, and intracorneal bacterial colonies
2. Head, dam, bone marrow, meninges, subdural space: Lymphoma, leukemia.

Contributor's Comment: NOD.Cg-*Prkdc^{scid} Il2rg^{tm1Wjl}*/SzJ, mice, commonly referred to as NSG,

are a relatively new immunodeficient genotype that is becoming increasingly popular in biomedical research. NSG has a loss of function mutation in the IL-2 receptor gamma chain, bred onto the NOD-scid background. NSG mice are expected to be completely deficient in lymphocytes (B, T, and NK cells), have undetectable serum Ig, and disrupted cytokine signaling. Their lack of NK function, lack of leakiness, lymphoma resistance, and relatively good breeding performance confer important advantages over scid, NOD-scid and nude mice. NSG mice are becoming increasing popular in studies involving tumor transplantation (solid or hematogenous), hematopoietic engraftment, and infectious and autoimmune diseases.[2,7] They are highly susceptible to opportunistic infections.

In the current case, histopathology of pups combined with PCR results confirmed infection with
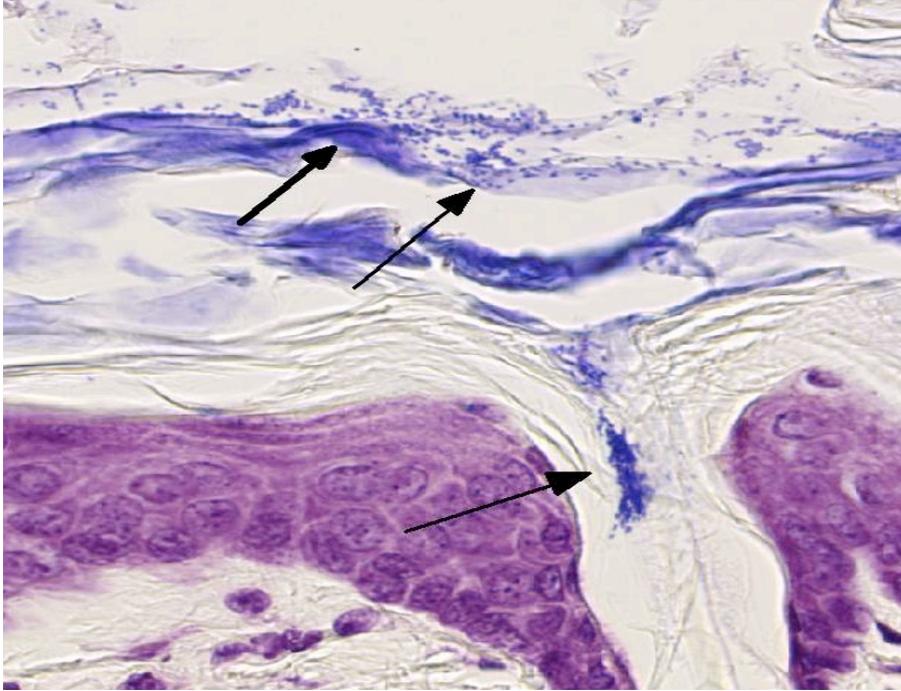
2-3. Haired skin, NSG mouse: Within the hyperkeratotic scale and concentrated within follicles, there are numerous gram-positive 2-3 μm rod-shaped bacilli consistent with Corynebacterium bovis. (Gram 400X)

Corynebacterium bovis in this NSG colony. The section on this slide is from the worst affected of the 2 dams. *Corynebacterium bovis*, the agent of "scaly skin disease" in mice, is a commensal and opportunistic bacterial agent that causes hyperkeratosis, pup mortality, and failure to thrive in susceptible mouse strains including immunodeficient nude, NOD SCID, and NSG mice.[1,2,3,7] Morbidity can be high, as transmission and persistence in the environment are associated with shedding of the infected keratin flakes.[8] Mortality is generally low, except in young/suckling mice.[8] Some immunocompetent mice may develop skin disease, but often harbor the bacteria without clinical signs, and thus serve as a reservoir, making it difficult to eradicate. Additionally, bacteria can persist in the environment, and can spread through sloughed keratin debris to other cage mates, or iatrogenically through handlers, which serve as a vehicle for transmission.[1,8] In addition to *C. bovis* infection, histologic evaluation of the gastrointestinal tract revealed a diverse enteric flora, including protozoa, corroborating the conventional microbial status of these animals. These findings strongly suggest that severely immunodeficient NSG mice require more stringent barrier conditions and microbial exclusion in order to thrive and be useful for research purposes.[10] The very mild dermatitis here was characterized as non suppurative, instead of lymphocytic or lymphoplasmacytic, because mice this genotype are expected not to have lymphocytes.
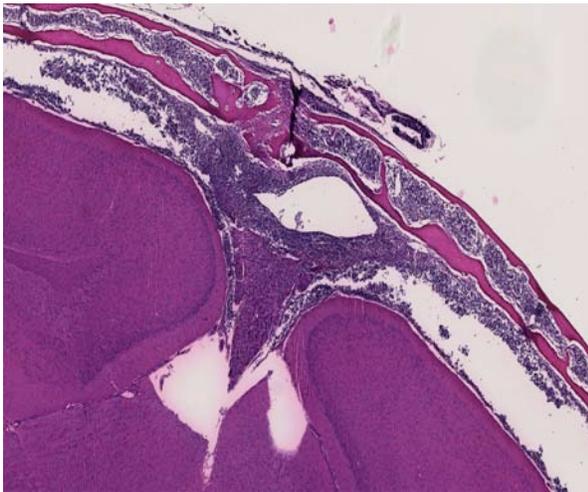
2-4. A cross section of the skull demonstrates an infiltrate of neoplastic lymphocytes within the meninges and also infiltrating the marrow spaces of the overlying cranium. (HE 48X)
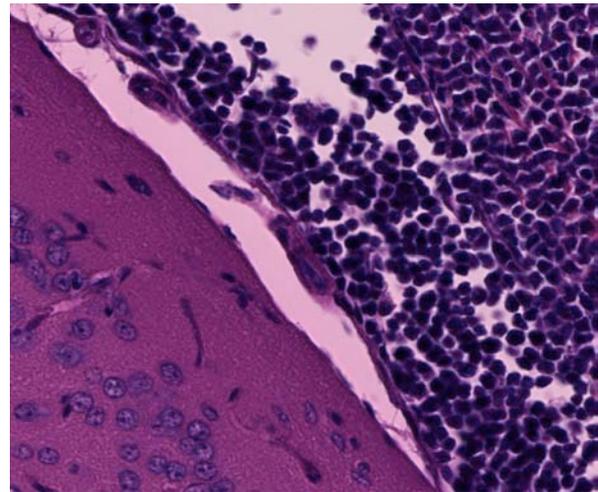
2-5. Unfortunately, decalcification of the section precludes detailed analysis of cytomorphology of the neoplastic lymphocytes in the sections received by conference participants. (HE 400X)

Interestingly, both submitted dams from this small group of breeding NSG mice had disseminated lymphoma with marrow and vascular involvement (leukemia). The head section is from Dam A. Cytomorphology, which is easier to assess in non-decalcified tissues, was consistent with a lymphoblastic lymphoma. Immunohistochemistry (on Dam A) was positive for CD3 and CD43, and negative for B220 and PAX5. These findings are consistent with T cell lymphoblastic lymphoma.[6] A similar presentation of lymphoma has been reported in the NOD.Cg-*Prkdc*[scid] *Il2rg*[tm1Sug]/JicTac mouse, sometimes called NOG, which is also on a NOD.scid background but has a different loss of the function mutation in Il2rg.[5] These findings represent the first documented reports of lymphoma in NSG mice, which have been considered to be completely lymphocyte deficient, resistant to lymphocyte 'leakiness' and resistant to lymphoma.[7] Immune stimulation associated with *Corynebacterium bovis* and other agents encountered with less stringent barrier conditions may predispose to lymphoma, and may compromise the research value and lifespan of immunodeficient mice.

JPC Diagnosis: 1. Haired skin: Hyperkeratosis, orthokeratotic, diffuse, moderate, with moderate epidermal hyperplasia and intracorneal bacilli.
2. Head, at level of hippocampus, cranial bone marrow, meninges, and tissues ventral to brain: Lymphocytic leukemia.

Conference Comment: Conference participants found this first report of lymphoma in NSG mice, so well described by the contributor, to be particularly interesting. While speculating on possible mechanisms, several questions arose, including the following: Could these neoplastic cells have arisen from a monocytic precursor? If so, what triggered the differentiation that resulted in expression of the identified markers? Are the circulating lymphocytes functional? It will be interesting to see future developments or any further reports of similar lesions in other NSG mice.

The use of various stains of *scid* mice in biomedical research originated from four littermates of the C.B-17 inbred strain that were found to lack IgM, IgG1, and IgG2a during a serum immunoglobulin quantitation study in 1983. These mice lacked both T and B lymphocytes because of a heritable recessive mutation, similar to a condition reported in humans.[9] *Scid* mice have a spontaneous loss-of-function mutation of the protein kinase, DNA activated, catalytic polypeptide (*Prkdc*) gene. Prkdc plays a role in repairing double-stranded DNA as well as in recombining the variable (V), diversity (D) and joining (J) segments of immunoglobulin and T cell receptor genes. Because of their inability to complete V(D)J gene recombination, T and B cells cannot mature; thus affected animals cannot develop cell mediated or humoral immune responses.

The penetrance of the *scid* mutation varies, and reduced penetrance can result in animals that are "leaky," developing immunoglobulin and T and B cells as they age.[3] Approximately 15% of *scid* mice have detectable serum Ig and functional T cells, and 15% of aged C.B17/Icr-*scid/scid* mice and 67% of 40-week-old NOD *scid/scid* mice develop thymic T-cell lymphomas.[9] Thus, as the contributor states, NSG mice, which are generally resistant to such "leakiness" are becoming increasingly popular in research. Nonetheless, the contributor provides a compelling argument that exposure to opportunistic pathogens may both circumvent the strain's natural resistance to leakiness, and contribute to the development of lymphoma; this case, therefore, underscores the importance of maintaining strict barrier conditions and microbial exclusion to preserve the research value of immunodeficient mice.

The relatively non-specific JPC histologic diagnosis of "lymphocytic leukemia" is based on the evaluation of hematoxylin- and eosin-stained sections available to conference participants. We believe that this diagnosis is attainable by conference participants; a more specific diagnosis of T-cell lymphoblastic leukemia would be appropriate if participants had access to non-decalcified sections and immunohistochemical studies performed by the contributor.

Contributing Institution: The Department of Molecular and Comparative Pathobiology
Johns Hopkins University
School of Medicine
733 N. Broadway St., Suite 811
Baltimore, MD 21205
http://www.hopkinsmedicine.org/mcp/index.html

References:
1. Burr HN, Lipman NL, White JR, Zheng J, Wolf FR. Strategies to prevent, treat, and provoke *Corynebacterium*-associated hyperkeratosis in athymic nude mice. *Journal of American Association for Laboratory Animal Science.*

2011;50:378-388.

2. Foreman O, Kavirayani AK, Griffey SM, Reader R, Shultz LD. Opportunistic bacterial infections in breeding colonies of the NSG mouse strain. *Vet Pathol.* 2011;48:495-499.

Jackson Laboratory Mouse Strain Data. *Scid* mice overview. http://jaxmice.jax.org/support/straindata/ scid.html. Accessed 2 March 2013.

3. Jacoby RO, Fox JG, Davidson M. Biology and diseases of mice. In: Fox JG, Anderson LC, Loew FM, Quimby FW, eds. *Laboratory Animal Medicine.* 2nd ed. San Diego, CA; Elsevier Science. 2002:92-93.

4. Kato C, Fujii E, Chen YJ, Endaya BB, Matsubara K, Suzuki M, et al. Spontaneous thymic lymphomas in the non-obese diabetic/Shi-scid, IL-2R γ^{null} mouse. *Laboratory Animals.* 2009;43:402-404.

5. Morse HC, Anver MR, Fredrickson TN, Haines DC, Harris AW, Harris NL, et al. Bethesda proposals for classification of lymphoid neoplasms in mice. *Blood.* 2002;100:246-258.

NOD.Cg-Prkdc^{scid} Il2rg^{tm1Wjl}/SzJ. The Jackson Laboratory. Bar Harbor, ME. http://jaxmice.jax.org/ literature/factsheet/SFS0001_005557.pdf, 2010

6. Scanziani E, Gobbi A, Crippa L, Giusti AM, Pesenti E, Cavalletti E, et al. Hyperkeratosis-associated coryneform infection in severe combined immunodeficient mice. *Laboratory Animals.* 1998;32:330-336.

7. Sudenberg JP, Shultz LD. The Severe Combined Immunodeficiency (scid) Mutation. JAX® Notes. 1993: 453. http://jaxmice.jax.org/jaxnotes/archive/ 453a.html. Accessed online on 2 March 2013.

8. Treuting PM, Clifford CB, Sellers RS, Brayton CF. Of mice and microflora: considerations for genetically engineered mice. *Veterinary Pathology.* 2012;49:44-63.

CASE III: 08-076G (JPC 3144240).

Signalment: Three-week-old, male, Mox-2 Cre transgenic mouse *(Mus musculus)*.

History: A mass was noted on left front leg.

Gross Pathologic Findings: A firm mass encompassed the left front leg from the shoulder to the paw (~2 cm in diameter).

Histopathologic Description: A cross-section of the left forelimb has an unencapsulated, expansile, and infiltrative mass expanding the dermis, extending into the subcutis, and replacing skeletal muscle. The mass is composed of densely-packed neoplastic cells haphazardly arranged as long and short interweaving streams and bundles within a minimal fibrovascular matrix. Neoplastic cells are predominantly spindle-shaped with some ovoid profiles; have abundant granular to fibrillar amphophilic cytoplasm; and prominent round to oval nuclei with marginalized chromatin and multiple magenta nucleoli. Many of these cells are quite long with a fairly consistent width, and fusiform nuclei (presumed strap cells). Neoplastic cells exhibit marked anisocytosis, anisokaryosis, and pleomorphism. Mitoses are numerous, varying between ~2 to ~10 per high-power field (40x). Multinucleated giant cells with abundant eosinophilic cytoplasm and 2 to 5 nuclei clustered at the periphery are frequently present (racket cells). Multifocal areas of the neoplasm are necrotic with hemorrhage and copious cytoplasmic and karyorrhectic debris. Small bundles of skeletal muscle entrapped by neoplastic cells are present at the periphery of the mass adjacent to sections of cortical bone. Mild edema (clear spaces) and moderate aggregates of lymphocytes and plasma cells multifocally expand the superficial dermis. The overlying epidermis has multiple variably sized ulcers with replacement by moderate amounts of degenerate neutrophils and eosinophilic debris. Small pockets of degenerate neutrophils are occasionally apparent within the stratum corneum.

Contributor's Morphologic Diagnosis: Left forelimb, skeletal muscle: Rhabdomyosarcoma.

Contributor's Comment: Spontaneous rhabdomyosarcomas in mice are rare with those of skeletal muscle occurring more often than those of the heart.[6] Rhabdomyosarcomas are typically induced experimentally via exposure to a variety of viruses, metals, and/or chemical carcinogens.[6] An investigation at the Jackson Laboratory identified 14 spontaneous well-differentiated rhabdomyosarcomas out of 10,000 mice, approximately 4 months old.[7] Landau et al[3] found a higher incidence of rhabdomyosarcomas (34% of controls); however, these mice were approximately 14 months old.

The mouse currently described was transgenic for the Mox-2 gene, which is an important regulator of vertebrate limb myogenesis.[4,8] Mox-2 is part of a cohort of genes important to normal myogenic
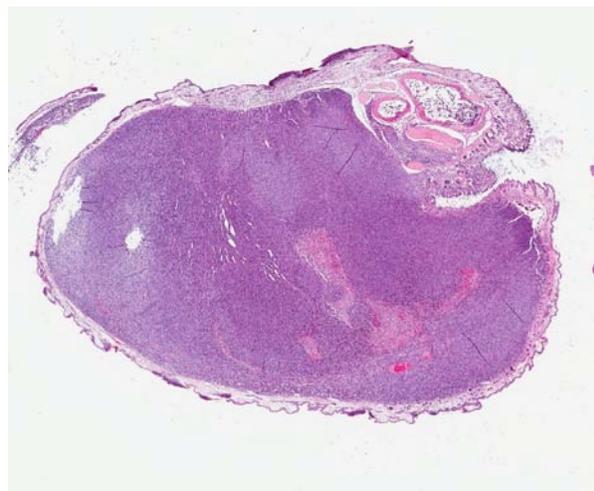
3-1. Left forelimb, Mox-2 Cre transgenic mouse: The limb is expanded up to 10 times normal diameter by an infiltrative mesenchymal neoplasm. (HE 40X)
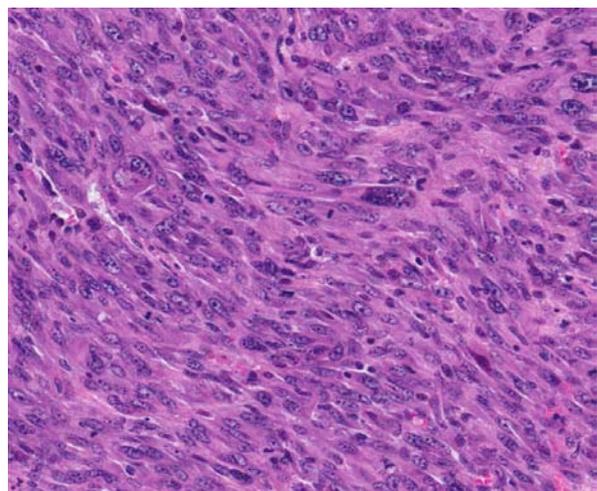
3-2. Left forelimb, Mox-2Cre transgenic mouse: The neoplasm is composed of mildly pleomorphic spindle cells arranged in broad streams. Neoplastic cells exhibit occasionally large nuclei, and often multiple nuclei arranged along the long axis of the cell. Mitotic figures are common. (HE 320X)

differentiation. Historically, mice homozygous for a null mutation of Mox-2 have a developmental defect of the limb musculature, characterized by an overall reduction in muscle mass and elimination of specific muscles (www.jax.org).

Identification of strap cells may be difficult by light microscopy; however, phosphotungstic acid-hematoxylin (PTAH) stain is useful for identification of cross-striations.[6,5] Malignant fibrous histiocytoma and leiomyosarcoma are differential diagnoses for rhabdomyosarcoma.[6] Immunolabels useful for differentiating these neoplasms include pan myosin, sarcomeric actin, desmin, actin, myosin, and smooth muscle actin.[7] The most useful antibodies are those that react with sarcomeric or smooth muscle actin.

JPC Diagnosis: Skeletal muscle, left forelimb: Rhabdomyosarcoma.

Conference Comment: Rhabdomyosarcomas (RMS) occur infrequently in domestic animals, as they do in mice. A recent publication reviewed the classification and pathogenesis of this diverse group of rare tumors, comparing canine rhabdomyosarcomas with those that occur in humans and with other canine soft tissue sarcomas.[1] Although in veterinary medicine rhabdomyosarcomas are often categorized as high grade soft tissue sarcomas, they are excluded from the soft tissue sarcoma grading scheme as recently proposed by Dennis et al.[2]

Diagnosis and classification is difficult due to their variation in phenotype, cellular morphology and age of onset. It is likely that some RMS are diagnosed as "undifferentiated sarcomas", "anaplastic sarcomas" or " poorly differentiated sarcomas", since skeletal muscle differentiation is not always evident by light microscopy. Therefore, immunohistochemistry can aid in the diagnosis. In addition to the immunolabels discussed by the contributor, MyoD1 and myogenin (early embryological transcription factors involved in mesoderm cell differentiation into myoblasts, myoblast proliferation and myoblast differentiation into myotubules) are associated with RMS of more undifferentiated cells.

Transmission electron microscopy can also aid in the diagnosis; however, EM is not helpful in classification, as several subtypes exhibit similar subcellular structures, including Z-lines, numerous mitochondria, myofilament tangles, and myosin-ribosome complexes.[1]

Canine classification of RMS is similar to the human classification of RMS, with the following subclasses:

- Embryonal, in which cells occur in different stages of development (from myoblast to myotubular) on a mucinous stroma. These occur in both juveniles and adults, and occur more frequently on the face, skull, within masticatory muscles, the oropharynx, trachea, axilla, scapula, perirenal, tongue, flank, leg, mammary gland, and hard palate. In the myotubular variant of embryonal RMS myotubule forms predominate; whereas large myoblast cells predominate in the rhabdomyoblastic variant and streams of plump spindle cells predominate in the spindle cell variant.[1]
- Botryoid RMS have a characteristic submucosal location and gross appearance that resembels grape-like masses. Histologically they appear as mixed round, undifferentiated myoblast cells and multinucleated myotubular cells on a mucinous stroma. These tend to occur in the urinary bladder or uterus in juveniles.[1]
- Alveolar RMS occur in juveniles and are usually found in the hip, maxilla, greater omentum or uterus. The classic variant is characterized by fibrous bands that divide small round cells into clusters and loose aggregates, while the solid variant is composed of closely packed cells with or without a thin fibrous septa.[1]
- Pleomorphic RMS typically occur in adult skeletal muscle. They are characterized by haphazardly arranged plump spindle cells with marked anisocytosis and anisokaryosis and bizarre mitotic figures.[1]

More studies are needed to determine if these classifications have prognostic significance in veterinary medicine.[1]

Contributing Institution: National Institute of Environmental Health Sciences
P.O. Box 12233
Research Triangle Park, NC 27709
http://ntp-server.niehs.nih.gov/

References:
1. Caserto BG. A comparative review of canine and human rhabdomyosarcoma with emphasis on classification and pathogenesis. *Vet Pathol Online*

First. Published online 25 February 2013. Accessed online 2 March 2013.

2. Dennis MM, McSporran KD, Bacon NJ, Schulman FY, Foster RA, Powers BE. Prognostic factors for cutaneous and subcutaneous soft tissue sarcomas in Dogs. *Vet Pathol.* 2011;48(1):73-84.

3. Landau JM, Wang ZY, Yang GY, Ding W, Yang CS. Inhibition of spontaneous formation of lung tumors and rhabdomyosarcomas in A/J mice by black and green tea. *Carcinogenesis.* 1998;19:501-507.

4. Mankoo BS, Collins NS, Ashby P, Grigorieva E, Pevny LH, Candia A, et al. Mox2 is a component of the genetic hierarchy controlling limb muscle development. *Nature*. 1990;400:69-73.

5. Leininger JR. Skeletal muscle. In: Maronpot RR, ed. *Pathology of the Mouse.* St. Louis, MO; Cache River Press. 1999;640-642.

6. Mohr U, ed. *International Classification of Rodent Tumors, The Mouse*. Berlin, Heidelberg: Springer-Verlag. 2001;385, 386.

7. Sundberg JP, Adkison DL, Bedigian HG. Skeletal muscle rhabdomyosarcomas in inbred laboratory mice. *Veterinary Pathology*. 1991;28:200-206.

8. Tiffin N, Williams, RD, Robertson D, Hill S, Shipley J, Pritchard-Jones K. WT1 expression does not disrupt myogenic differentiation in C2C12 murine myoblasts or in human rhabdomyosarcoma. *Experimental Cell Research*. 2003;287:155–165.

CASE IV: N47/09 (JPC 3149877).

Signalment: 8-year-old, castrated male, domestic short hair, feline *(Felis domesticus)*.

History: This cat was referred to the University Veterinary Hospital, University College Dublin with a two-month history of weight loss. It presented with periorbital alopecia, nasal discharge, pale mucus membranes and a heart murmur. Blood tests revealed a severe non-regenerative anaemia, neutropaenia and thrombocytopaenia.

Gross Pathologic Findings: The cat presented in poor body condition with pale mucus membranes. Focal areas of alopecia extended over both upper eyelids to the bases of both ears, and red crusted lesions were present over the upper eyelids and lateral canthuses (more extensive on the right). The right third eyelid was thickened and erythematous as were the nasal conchae. The nasal planum, particularly on the right, had a dry, crusty and flaky appearance. There was a small amount of serohaemorrhagic pericardial fluid. The mesenteric lymph nodes were enlarged and on sectioning contained mottled red and pale pink areas. The bone marrow was dark red in color and filled the marrow space.

Histopathologic Description: Multifocal ulcers covered by serocellular crust are present on the anterior surface of the eyelid. There is a moderate perifollicular and mural follicular inflammatory infiltrate consisting of macrophages, occasional neutrophils, lymphocytes and plasma cells along with a large numbers of mast cells. Hair follicles often contain mites. Multiple large areas of ulceration covered by a serocellular crust are apparent on the conjunctival surface of the eyelid and moderate neutrophilic and lymphocytic infiltration is apparent in the underlying mucosa. Epithelial cells immediately adjacent to the ulcerated areas are enlarged and occasionally contain large eosinophilic to amphophilic intra-nuclear inclusion bodies with marginated chromatin. There are accompanying necrotic 'ghost' epithelial cells. Additional histological lesions include an ulcerative lymphoplasmacytic rhinitis and bone marrow hypercellularity with a reduced erythroid ratio (not submitted).

Contributor's Morphologic Diagnosis: 1. Severe acute ulcerative conjunctivitis with intralesional intranuclear inclusion bodies consistent with feline herpesvirus infection.
2. Subacute ulcerative folliculitis with intralesional mites suggestive of *Notoedres cati.*

Contributor's Comment: Feline herpesvirus 1 (FHV-1) is a common, worldwide infection of domestic cats of high morbidity and low mortality. A member of the alphaherpes virus subfamily, latency often develops after infection.[2,6] Up to 90% of tested cats are seropositive for this virus.[6]

Most cats are infected as kittens, developing conjunctivitis, corneal ulceration or rhinitis of varying severity depending on viral strain and host susceptibility. The virus replicates in epithelial cells at temperatures below 37° Celsius and so its

4-1. Eyelid, cat: Foci of ulceration (arrows) are present within both the haired skin and conjunctival surface of the eyelid. (HE 4X)
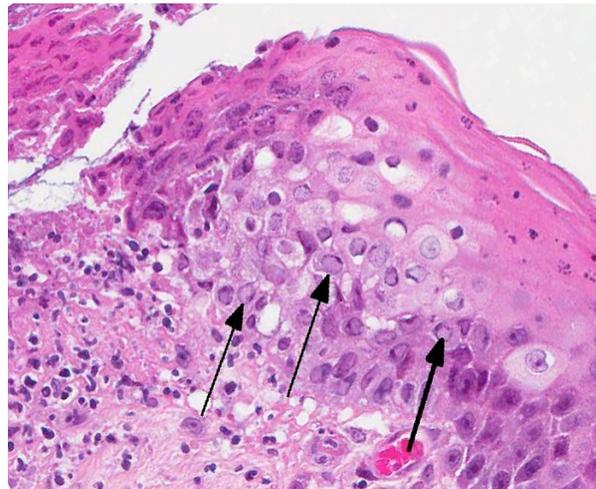
4-2. Eyelid, conjunctival surface: At the edge of an area of ulceration, mucosal epithelial nuclei are enlarged by a smudgy, amphophilic intranuclear viral inclusion. (HE 400X)
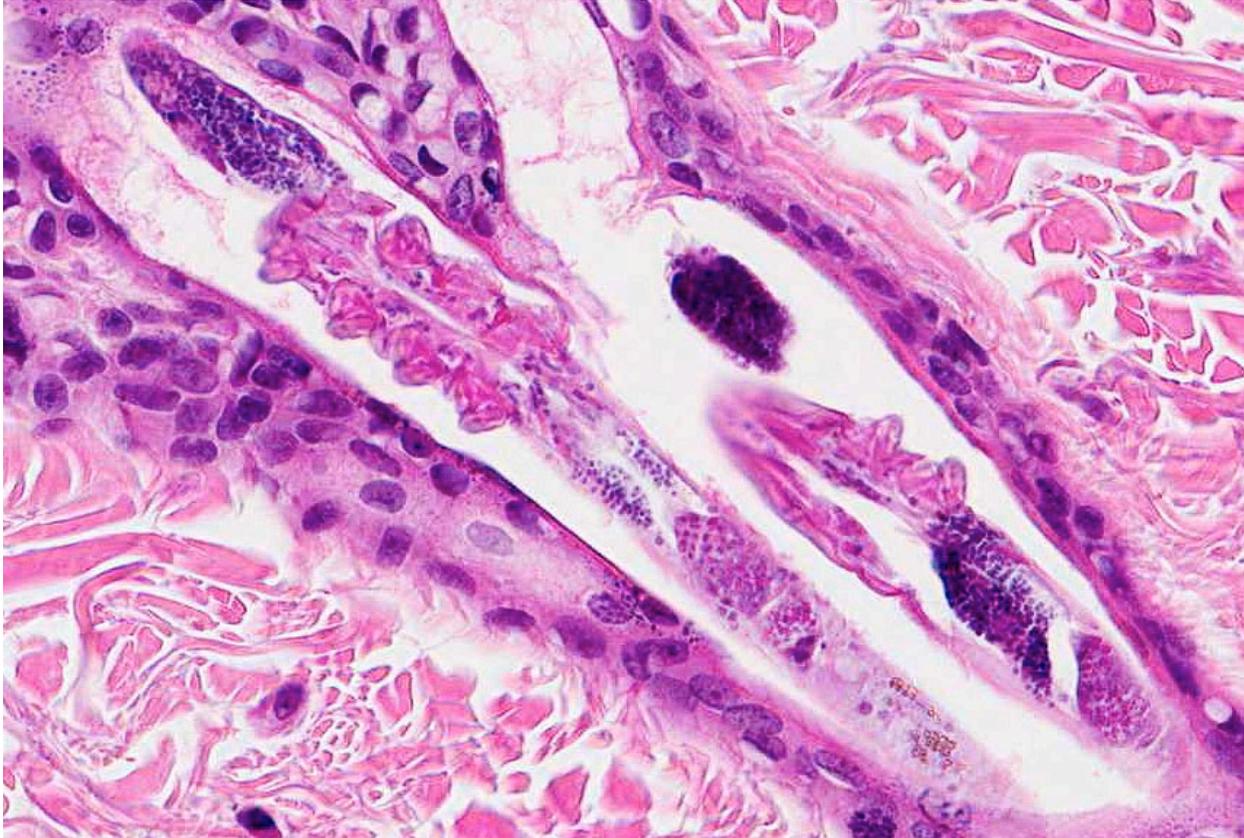
4-3. Eyelid, haired skin: Hair follicles contain one to multiple cross sections of an elongate, cigar-shaped arthropod paraside with chitinous exoskeleton, jointed appendages, and skeletal muscle, consistent with Demodex cati. (HE 400X)

preferential proliferation sites are peripheral locations such as ocular and nasal mucosa. The virus damages tissue by direct cytolysis during replication and secondarily by immune-mediated inflammation. Cytolysis results in corneal ulceration, conjunctivitis with ulceration and rhinitis with erosions. Immune-mediated injury is less common and results in stromal keratitis. In primary infections the most common presenting lesion is conjunctivitis.[2,7]

Up to 80% of infected cats go on to develop virus latency, typically in the trigeminal nerve, from which latency associated transcripts of FHV-1 have been demonstrated. More recently, evidence of persistent low-grade viral infection has been demonstrated in the cornea.[2,6,7] In approximately 50% of carriers, reactivation of infection can occur either spontaneously or during periods of stress or corticosteroid administration. Classically, this is associated with centrifugal spread of the virus from the trigeminal nerve along the sensory nerves to the original epithelial site of invasion. Upon reactivation, viral shedding recommences and this can be with or without recrudescence of clinical signs. With reactivation, the most common presenting clinical sign is conjunctivitis.[2]

Notoedres cati (feline scabies) is a rare, highly contagious ectoparasite of cats causing alopecia with adherent crusts around the head and ears, particularly the ear pinna. Histologically the parasite triggers superficial dermatitis with eosinophil-rich perivascular inflammation.[3]

JPC Diagnosis: 1. Eyelid: Blepharoconjunctivitis, ulcerative, focally extensive, severe with intranuclear viral inclusions.
2. Haired skin, eyelid follicles and sebaceous glands: Adult arthropod parasites, etiology consistent with *Demodex cati*.

Conference Comment: The contributor provides an excellent review of feline herpesvirus-1. Conference participants discussed the three most common clinical differential diagnoses for upper respiratory disease in cats, specifically feline viral rhinotracheitis (caused by FHV-1), feline calicivirus

rhinitis (caused by feline calicivirus) and feline chlamydiosis (caused by *Chlamydophila felis*).[5] In general, feline viral rhinotracheitis manifests clinically as rhinitis, conjunctivitis and/or ulcerative keratitis; whereas, feline calicivirus often causes rhinitis, conjunctivitis, ulcerative gingivitis and stomatitis[5] and signs of *Chlamydophila felis* infection are often limited to rhinitis and conjunctivitis. Participants noted that these differences in presentation can be helpful in making a clinical diagnosis.

Dr. Chris Gardiner, JPC consultant in veterinary parasitology, believes these arthropods are more consistent with *Demodex* rather than *Notoedres cati* and provided by following justification: "…The mites in this specimen are elongate and found within the hair follicles; whereas, *Notoedres cati* mites are dorsoventrally flattened, similar to other members of the Family *Sarcoptidae,* and are typically observed in the stratum corneum.[1,4] Additionally, *Demodex* spp. are the only parasitic mites in which all four pairs of appendages originate together. *Notoedres* mites, on the other hand, have two pairs of two appendages that originate together separated by a space from another two pairs of two appendages that originate together." (C.H. Gardiner, personal communication).

Contributing Institution: UCD Veterinary Sciences Centre
UCD School of Agriculture
Food Science and Veterinary Medicine
University College Dublin
Belfield, Dublin 4
Ireland
www.ucd.ie

References:
1. Bowman, DD. Arthropods. In: *Georgis' Parasitology for Veterinarians.* 9th ed. St. Louis, MO: Saunders Elsevier; 2009:64-66.
2. Gaskell R, Dawson S, Ramford A, Thiry E. Feline herpesvirus. *Vet Res*. 2007;38:337-354.
3. Ginn PE, Mansell JEKL, Rakich PM. Skin and appendages. In: Maxie MG, ed. Jubb, Kennedy and Palmer's Pathology of Domestic Animals. 5th ed. vol. 1. Philadelphia, PA: Elsevier Saunders; 2007:721-722.
4. Hargis Am, Ginn PE. The integument. In: Zachary JF, McGavin MD, eds. *Pathologic Basis of Veterinary Disease.* St. Louis MO: Elsevier Mosby; 2012:1043.
5. Lopez A. Respiratory system, mediastinum, and pleurae. In: Zachary JF, McGavin MD, eds. *Pathologic Basis of Veterinary Disease.* St. Louis MO: Elsevier Mosby; 2012:473.
6. Maggs DJ. Update on pathogenesis, diagnosis and treatment of feline herpesvirus type 1. *Clin Tech Small Anim Pract*. 2005;20:94-101.
7. Wilcock BP. Eye and ear. In: Maxie MG, ed. *Jubb, Kennedy and Palmer's Pathology of Domestic Animals.* 5th ed. vol. 1. Philadelphia, PA: Elsevier Saunders; 2007:490-491.